Quantification of Osteon Morphology Using Geometric Histomorphometrics

Dillon, Scott; Cunningham, Craig; Felts, Paul

Published in:
Journal of Forensic Sciences

DOI:
10.1111/1556-4029.12966

Publication date:
2016

Document Version
Peer reviewed version

Journal of Forensic Sciences

Technical Note Submission

"Quantification of osteon morphology using geometric histomorphometrics"

Mr Scott Dillon (M.Sci.), Dr Craig Cunningham (Ph.D.) and Dr Paul Felts (Ph.D.)

Centre for Anatomy and Human Identification

College of Art, Science and Engineering

University of Dundee

Medical Sciences Institute

Dow Street

Dundee

DD1 5EH

ABSTRACT: Many histological methods in forensic anthropology utilise combinations of traditional histomorphometric parameters which may not accurately describe the morphology of microstructural features. Here we report the novel application of a geometric morphometric method suitable when considering structures without anatomically homologous landmarks for the quantification of complete secondary osteon size and morphology. The method is tested for its suitability in the measurement of intact secondary osteons using osteons digitised from transverse femoral diaphyseal sections prepared from two human individuals. The results of methodological testing demonstrate the efficacy of the technique when applied to intact secondary osteons. In providing accurate characterisation of micromorphology within the robust mathematical framework of geometric morphometrics, this method may surpass traditional histomorphometric variables currently employed in forensic research and practice. A preliminary study of the inter-sectional histomorphometric variation within the femoral diaphysis is made using this geometric histomorphometric method to demonstrate its potential.

KEYWORDS: forensic science, forensic anthropology, bone histology, geometric morphometrics, histomorphometrics, human identification

The qualitative and quantitative histological examination of the skeleton has found useful application in a number of sub-disciplines within forensic anthropology, such as in human/non-human (H/N-H) determination (1) and age estimation (2). The histological features of bone are influenced by development, the remodelling process and the principal of bone functional adaptation, leading to variation in the size, shape or distribution of microstructural units or tissue types (3-5). These features may be exploited when attempting to determine whether a bone (or bone fragment) is human, or the age of an individual at the time of death. Many authors within the scientific literature have expounded upon the virtues of histological techniques in instances in which the forensic anthropologist is confronted with incomplete sets of remains (a single femur for example), fragmentary human remains, or unidentified fragmentary remains, of both dental (6) and skeletal (7) origin. In these instances histological techniques and methods may allow the anthropologist to establish forensic context (as with H/N-H determination), or provide an estimation for part of the biological profile which would otherwise be unobtainable given the preservation state of the remains. Franklin (7) also notes that histological age estimation standards are available in a wide range of skeletal elements which include acceptable margins of error, thus enabling the application of histological methods in a variety of forensic situations.

A wide range of methods have been published to facilitate both H/N-H determination and age estimation from cortical bone histology. One current problem associated with these methods however is the wide variety of histomorphometric parameters which have been used to quantify aspects of the bone microstructure and its units. Absolonova and colleagues (8) for example employed a comprehensive series of 28 parameters to measure secondary osteon and Haversian canal morphology, along with other features of the cortical microstructure in human ribs. Other authors however have utilised highly variable permutations of these and other parameters within their own studies to quantify aspects of the same structures. Two

complications arise from this. Firstly, the use of multiple traditional measures of size and morphology (e.g. osteon area and minimum/maximum diameter) will inevitably lead to a degree of overlap in the histomorphometric variation measured by each. Given that different combinations of parameters are employed by individual authors, it is difficult to know what degree of redundancy is introduced into the data, and which combinations of parameters are most efficient in capturing variation. Secondly, it is not known whether traditional histomorphometrics (THMM) are able to adequately describe all biologically meaningful variation in the size and morphology of histological structures. Osteon circularity for instance provides a measure of shape, but assumes that osteons may be modelled on a scale of transformation between a perfect circle and an increasingly elongated ellipse (9). These issues do not affect histological age estimation with the same significance as H/N-H determination as the preference is to use osteon population counts rather than direct measurement of morphology (10). However, many methods of H/N-H determination continue to employ THMM measures of osteon and Haversian canal morphology (9, 11-15).

Geometric morphometric (GMM) methods and statistics have become increasingly popular within biology in recent years due to their ability to preserve and analyse the spatial relationships between anatomical constructions, thus providing an unbiased measure of both the size and shape of structures (16-19). GMM methodologies use configurations of anatomical landmarks, described using Cartesian co-ordinates, to record information about the relative spatial positions of these points in either 2- or 3-dimensions. This data may then be subject to superimposition methods (such as generalised Procrustes analysis; GPA) to remove all information relating to position, rotation and scale, thereby preserving only information relevant to the shape of specimens. GMM measurements of shape are therefore multivariate by definition and statistical analysis is often based upon the use of techniques which reduce dimensionality, such as principal component analysis (PCA) or canonical variate analysis

(CVA). Shape may then be represented by a single value upon each principal or canonical axis. The 'size' of structures in GMM is measured using the centroid size variable. This is calculated as the square root of the sum of the squared Euclidean distances between each landmark and the centroid of the configuration (16-18). This method of size computation results in values which are independent of shape. Consequent separation allows the independent analysis of size and shape, along with the relative contributions of these variables to the morphological variation of specimens. See reviews by Webster and Sheets (17) and Viscosi and Cardini (18) for an introduction to GMM theory with illustrative examples.

Despite these advantages, geometric morphometrics has not yet been applied to the measurement of osteon or Haversian canal morphology. This is in part due to the absence of biologically homologous landmark points (either topographically or functionally homologous) between any two given osteons, preventing the use of more widespread landmark-based GMM methods (18). Such methodologies identify and digitise a number of points around or upon a structure based upon anatomical landmarks. In subsequent analyses, corresponding landmark points are treated as homologous to one another across specimens. While many outline methods are available which do not depend on homologous points (16, 20), the versatility of landmark-based methodologies provides many advantages in the description, analysis and visualisation of shape data - see (21) for a full discussion.

The aim of this paper therefore is to report the novel application of a geometric morphometric method to the measurement of secondary osteon morphology, using a landmark-independent Fourier analysis method based on that of Ferretti *et al* (22) and utilising the improved Fourier shape analysis protocol of Haines and Crampton (23). This methodology allows the subsequent analysis of data using landmark-based methods. Furthermore, this paper will demonstrate the potential use of this method in the analysis of the inter-sectional histomorphometric variation of osteons within diaphyseal cortical bone.

Materials and Methods

All samples of human bone utilised within this study were taken from 2 left femora, as harvested from cadavers within the dissecting room at the Centre for Anatomy and Human Identification (CAHID), University of Dundee. Both individuals were female and aged 87 (Individual 1) and 88 (Individual 2) respectively. Tissue collection was performed as part of a larger project and with the approval of the CAHID ethics board.

Cross-sectional blocks of approximately 2cm in width were cut transversely at 3 diaphyseal sampling sites using a hacksaw. Sites were designated as the metric midshaft of the femur (as measured from the physiological length of the bone), the proximal site (a third of the physiological length from its proximal extremity) and the distal site (a third of the physiological length from its distal extremity). Relative rather than absolute determination of sampling sites allowed the maintenance of biomechanical homology between sites in bones of different lengths.

Thin sections suitable for transmitted light microscopy were cut from cross-sectional blocks using a Buehler® IsoMet™ 500 Linear Precision Saw. Relatively thick sections (~1mm) were initially cut from the surface of cross-sectional blocks to remove any striations caused by transverse sectioning. Thin sections (100-120µm in thickness) were then cut from the blocks before staining with the modified toluidine blue protocol developed by Osborne and Curtis (24) for demarcation of the cement lines. Thin sections were subsequently mounted on microscope slides using Histomount™ (National Diagnostics Inc.).

Micrographs of all fields at 4X magnification were captured using a Leitz Orthoplan light microscope along with a Leica® DFC295 (Leica Microsystems Ltd) microscope camera. The image acquisition system was calibrated using a stage micrometer prior to the beginning of the project. No image enhancement was performed. Individual micrographs were stitched

using The Stitching Plugin (25) available within the Fiji image analysis program (26) to produce a single high-resolution image of each entire cross-section.

The geometric histomorphometric protocol

Data processing between stages of the geometric histomorphometric (GHMM) protocol was achieved through use of custom Microsoft Excel macros (available from the authors) and text editing software. Complete secondary osteons (≥ 90% cement line intact) were initially manually outlined using a graphics tablet and pen (Turcom™) with the freeform selection tool within Fiji (26). These selections were filled to produce black objects and extracted from the original composite micrograph using Adobe® Photoshop® (Adobe Systems Inc.). Osteon objects were individually outlined using the recommended number of outline points within TPSDig2 (27). Fourier shape analysis according to the method constructed by Haines and Crampton (23) was employed, with use of the improved HTREE program and 5 smoothing iterations. This allows decomposition of outline data into Fourier harmonics and subsequent transformation of individual outlines to normalise for the starting point of digitisation with respect to the entire population of outlines. This effectively generates a dataset within which corresponding outline points may be treated as mathematically homologous, and thereafter may be treated as landmark points in subsequent analyses (23). Fourier shape analysis was performed using the Paleontological Statistics (PAST) software package (28). Individual osteon outlines were reconstructed using the program HCURVE (29). This allows the recomputation of Cartesian co-ordinates for each outline point from their Fourier harmonics. The number of outline points of which osteon outlines are composed was adjusted using Resample (30). The number of resampled points was informed by methodological testing (see below). The TPS data format was reconstructed to facilitate statistical analysis and data

visualisation. Finally, GPA was used to eliminate all non-shape related variation and centroid sizes were computed. Subsequent analyses were performed within MorphoJ (31) and PAST (28).

Development and testing of the geometric histomorphometric protocol

A number of initial analyses were carried out to assess the applicability of the Ferretti *et al* (22) technique to cortical bone histology. Firstly, efficacy of the starting point normalisation component of the HSHAPE software series (29) was tested when applied to secondary osteons. 10 intact secondary osteons were randomly selected from the midshaft cross-section of Individual 1 and repeatedly digitised using the recommended number of outline points and a random starting position 5 times within TpsDig2 (27). Each osteon group was labelled A-J. A complete dataset of all repeated digitisations was then subjected to the GHMM processing protocol. Procrustes distances between individual osteon repeat digitisations were calculated using PAST (28). Repeat group was used as the factor in a permutation ANOVA of Procrustes distances between repeated digitisation sets with 10,000 iterations to test for differences between sets of digitisation replications.

The ability of the GHMM protocol to detect differences between distinct osteons was also tested. Using the previous dataset of repeated digitisations, canonical variate analysis was performed along with a permutation test of pairwise group Procrustes distances between individual osteon groups with 10,000 iterations.

Finally, the degree of landmark resampling appropriate was tested. The output of the Fourier analysis method employed here describes each osteon outline with 1024 landmarks (29). While this is extremely detailed, this landmark configuration likely preserves minute

variation which is biologically meaningless and which will mask true shape fluctuation. The program Resample (30) was therefore used to reduce the number of landmarks constituting a given outline while retaining outline morphology. This is achieved through weighted linear interpolation. The previously analysed 10 osteons were each digitised once using the recommended number of outline points and subjected to the GHMM processing protocol. This was repeated both without resampling (1024 landmark configuration) and resampling to a 50 landmark configuration. Differences between the configurations were tested for using a Mantel matrix correlation test of Euclidean distances with 10,000 permutations. A bivariate Spearman's rho correlation was used to compute the correlation between centroid size values in the two landmark configurations.

The quantification of inter-sectional variation using geometric histomorphometrics

A novel sampling protocol which allowed unbiased identification of regions of interest was employed so as to incorporate the fullest extent of intra-sectional variation possible (see Figure 1). This is based upon the method proposed by Lynnerup *et al* (32), but modified so as to consider deviation in cortical thickness through use of relative, rather than absolute, width grids. All qualifying secondary osteons within extracted regions of interest were analysed using the GHMM protocol. As stated previously, these were the complete secondary osteons which retained ≥ 90% of their cement lines to facilitate accurate outlining. Osteons which exhibited irregular Haversian canals were also excluded so as to avoid collection of those which were not sectioned in the transverse plane. Due to the preliminary nature of this study, other categories of osteon were not considered, nor were resorption or void spaces. Reconstructed outlines were resampled according to the results of earlier sub-studies. Differences between sampling sites were elucidated using a canonical variate analysis of subsequent Procrustes co-

ordinates, including a permutation test of pairwise distances with 10,000 iterations. A permutation ANOVA with 10,000 iterations was also used to test for differences between groups in centroid size.

Results

Methodological testing

Repeated permutation ANOVAs revealed no statistically significant differences between groups of Procrustes distances as calculated from repeated osteon digitisations ($0.992 \leq p \geq 0.171$; see Table 1). Furthermore, canonical variate analysis paired with a permutation test of Procrustes distances between groups of osteons reported significant differences between all pairwise comparisons ($0.009 \leq p \geq 0.0001$; see Table 2). This allows us to confirm that firstly, the GHMM protocol is consistent in the characterisation of secondary osteon morphology to the point that no statistically significant differences are detectable between repeated osteon digitisations. Secondly, the canonical variate analysis/permutation test combination reveals that this methodology is also sensitive to differences in morphology between two distinct osteons.

The Mantel matrix correlation test applied to the 1024 and 50 landmark configurations reported a highly significant correlation of Euclidean distances between configurations, with an R value of 0.9998 ($p = 1.0x10^{-4}$). A highly significant correlation was also revealed between centroid size values using Spearman's rho ($R = 0.988$; $p < 0.001$). The resampled configuration therefore describes secondary osteon morphology as accurately as the 1024 configuration. Computation of centroid size is also unaffected by resampling.

Inter-sectional variation

544 secondary osteons were measured in total across both individuals. Table 3 details descriptive statistics for both shape data (in terms of canonical variate scores) and centroid size. Figure 2 displays Procrustes co-ordinates of all measured osteons regardless of sampling site with the spread of landmark positions around the mean of each of the 50 landmark points, along with the mean osteon shape within each sampling site. Canonical variate analysis with sampling site as a grouping variable produced two canonical axes explaining 100% of the sample variation. That is, all of the variation in shape between sampling sites may be described as a composite between these two axes of transformation. Figure 3 plots shape variation upon these axes, the extremes of which are defined using transformation grids as warped from the mean shape to illustrate change in secondary osteon morphology along a given axis. A permutation test of pairwise Procrustes distances between sampling site canonical variate scores revealed highly statistically significant differences between all pairs of sites (Table 4). This indicates that the change in shape of secondary osteons between sampling sites is considerable and that each sampling site may be characterised by distinct secondary osteon morphology.

On average, the size of osteons increased from proximal to distal sections, with the distal site exhibiting considerably larger osteons than the proximal or midshaft sites. Osteon size was extremely variable however, with the most consistent osteons present within distal sites (Table 3; Figure 4). A one-way permutation ANOVA reported statistically significant differences in centroid size between the distal site and the remaining two, but not between the midshaft and proximal sites (Table 5).

Discussion

This study has demonstrated firstly that the method developed by Ferretti and colleagues (22) using the Fourier shape analysis protocol of Haines and Crampton (23) can be used to accurately characterise the size and morphology of complete secondary osteons. This could easily be extended to other features of bone microstructure, such as Haversian canals or fragmentary osteons. In providing a comprehensive measure of osteon morphology, this method surpasses traditional histomorphometrics which may rely on a false assumption (as with osteon circularity), may only describe a very limited axis of change in shape and size per variable, or may introduce redundancy into the data with multiple measures of overlapping variation. This is demonstrated through the characterisation of shape variation between sampling sites in the diaphysis of the femur, the major axes of which defy any easy description of transformation between extremes (see Figure 3). It is therefore likely that some of this variation will escape quantification using limited traditional histomorphometric variables, although this is difficult to quantify directly. (In providing a measure of osteon size which is independent of osteon shape, this GHMM method will also allow researchers to explore the relative contributions of these factors to variation in osteon morphology, biological and anatomical influences which may affect these variables separately, and the forensic implications of this.)(*Scott: I am having trouble understanding this sentence after 'variation in osteon morpohology'. What are the 'biological and anatomical influences'? Is the part after 'factors to' a list with 3 items?) This may extend, for example, to whether cortical bone experiencing distinct biomechanical loading environments exhibits osteons with distinct adaptive shapes, and what relationship this has with osteon size. These investigations would have considerable potential in histological H/N-H determination.

Commented [S1]: Dr Felts – Sorry if this is ambiguous; it is indeed a list with three factors

Furthermore, we have here usefully applied the GHMM method to analyse inter-sectional variation in secondary osteon morphology. It should be noted that these analyses are for demonstrative purposes. The limited sample size, along with non-representative age and

sex distributions prevents interpretation of the trends exhibited here in terms of the general population. These patterns of variation are also not representative of any single point along the femoral diaphysis (aside from the midshaft), but rather compare sampling sites relative to one another, i.e. a comparison of biomechanical environments to each other. The results may however be interpreted in context with the surrounding scientific literature, especially as relating to osteon size.

Given a larger sample size, it would be possible using this protocol to characterise change in the size and shape of osteons throughout a given skeletal element, or a number of elements. Further potential analyses which may be facilitated through geometric histomorphometrics also include examining the relationship between osteonal shape and size, with respect to how this relationship is influenced by the local strain environment. Should this be combined with biomechanical data and other novel methodologies in bone histology – e.g. that developed by Rose *et al* (33) – it may be possible to model microstructural variation throughout the skeleton and its relationship with skeletal biomechanics, taking advantage of the robust mathematical framework provided by geometric morphometrics. Not only would this improve our anatomical knowledge in terms of how microstructural morphology changes with respect to the influence of mechanical factors upon the remodelling process, but may lead to the production of universal standards for H/N-H determination or age estimation which are not reliant on any given sampling site, as many current techniques are. Given that research has demonstrated the deleterious effect of cortical histomorphometric variation on the accuracy of methodologies based upon single sampling sites when applied outside those sampling sites (14, 34-36), the development of universal standards (or sets of standards which may be applied to range of sampling sites) is of critical importance. This is especially pertinent given the evolution in stringency of the legal rules regarding the admissibility of expert evidence in the United States (37, 38) and the proposal to bring similar regulations to the United Kingdom

(39). Universal discriminatory standards would therefore enable the scientifically and legally valid application of histological techniques in forensic anthropology to highly fragmented unidentified human bone or unidentified fragments of unknown origin. This could potentially provide a H/-NH determination or age estimation which would be impossible to obtain otherwise though more conventional morphological or osteometric analyses. Furthermore, histological techniques based upon universal standards would be founded within the well researched biological principle of bone remodelling, and would also be accompanied by a measureable margin of error.

Acknowledgements

The authors thank Valerie Wilson (School of Dentistry, University of Dundee) for technical support and Andrea Cardini (University of Modena and Reggio Emilia) for methodological assistance.

References

1. Hillier ML, Bell LS. Differentiating Human Bone from Animal Bone: A Review of Histological Methods. J Forensic Sci 2007;52(2):249-63.

2. Streeter S. Histological Age-at-Death Estimation. In: Crowder C, Stout S, editors. Bone Histology: An Anthropological Perspective. Boca Raton: CRC Press; 2012;135-52.

3. Ruff C, Holt B, Trinkaus E. Who's afraid of the big bad Wolff?: “Wolff's law” and bone functional adaptation. Am J Phys Anthropol 2006;129(4):484-98.

4. Robling AG, Stout SD. Histomorphometry of Human Cortical Bone: Applications to Age Estimation. Biological Anthropology of the Human Skeleton: John Wiley & Sons, Inc.; 2007;149-82.

5. Stout S, Crowder C. Bone Remodelling, Histomorphology, and Histomorphometry. In: Crowder C, Stout S, editors. Bone Histology: An Anthropological Perspective. Boca Raton: CRC Press, 2012;1-22.

6. Schmeling A, Geserick G, Reisinger W, Olze A. Age estimation. Forensic Sci Int 2007;165(2):178-81.

7. Franklin D. Forensic age estimation in human skeletal remains: Current concepts and future directions. Leg Med 2010;12(1):1-7.

8. Absolonova K, Veleminsky P, Dobisikova M, Beran M, Zocova J. Histological Estimation of Age at Death from the Compact Bone of Burned and Unburned Human Ribs. J Forensic Sci 2013;58:S135-S45.

9. Dominguez VM, Crowder CM. The utility of osteon shape and circularity for differentiating human and non-human Haversian bone. Am J Phys Anthropol 2012;149(1):84-91.

10. Stout SD, Stanley SC. Percent osteonal bone versus osteon counts: The variable of choice for estimating age at death. Am J Phys Anthropol 1991;86(4):515-9.

11. Cattaneo C, DiMartino S, Scali S, Craig OE, Grandi M, Sokol RJ. Determining the human origin of fragments of burnt bone: a comparative study of histological, immunological and DNA techniques. Forensic Sci Int 1999;102(2):181-91.

12. Urbanová P, Novotny V. Distinguishing between human and non-human bones: Histometric method for forensic anthropology. Anthropologie 2005;43(1):77-85.

13. Martiniaková M, Grosskopf B, Omelka R, Vondráková M, Bauerová M. Differences Among Species in Compact Bone Tissue Microstructure of Mammalian Skeleton: Use of a Discriminant Function Analysis for Species Identification. J Forensic Sci 2006;51(6):1235-9.

14. Cattaneo C, Porta D, Gibelli D, Gamba C. Histological Determination of the Human Origin of Bone Fragments. J Forensic Sci 2009;54(3):531-3.

Commented [S2]: Not sure how to cite this – Anthropologie does not have an Index Medicus abbreviation.

15. Crescimanno A, Stout SD. Differentiating Fragmented Human and Nonhuman Long Bone Using Osteon Circularity. J Forensic Sci 2012;57(2):287-94.

16. Adams DC, Rohlf FJ, Slice DE. Geometric morphometrics: Ten years of progress following the 'revolution'. Italian Journal of Zoology 2004;71(1):5-16.

17. Webster M, Sheets HD. A practical introduction to landmark-based geometric morphometrics. Quantitative Methods in Paleobiology Paleontological Society Papers 2010;16:163-88.

18. Viscosi V, Cardini A. Leaf Morphology, Taxonomy and Geometric Morphometrics: A Simplified Protocol for Beginners. PLoS One 2011;6(10):e25630.

19. Laitman JT, Albertine KH. The Anatomical Record by the Numbers: Seeing Anatomy Through the Lens of Mathematics and Geometry. Anat Rec 2015;298(1):1-2.

20. Bookstein FL. Landmark methods for forms without landmarks: morphometrics of group differences in outline shape. Med Image Anal 1997;1(3):225-43.

21. O'Higgins P. Methodological issues in the description of forms. In: Lestrel PE, editor. Fourier descriptors and their applications in biology. Cambridge: Cambridge University Press, 1997;74-105.

22. Ferretti A, Cardini A, Crampton JS, Serpagli E, Sheets HD, Štorch P. Rings without a lord? Enigmatic fossils from the lower Palaeozoic of Bohemia and the Carnic Alps. Lethaia 2013;46(2):211-22.

23. Haines AJ, Crampton JS. Improvements To The Method Of Fourier Shape Analysis As Applied In Morphometric Studies. Palaeontology 2000;43(4):765-83.

24. Osborne DL, Curtis J. A Protocol for the Staining of Cement Lines in Adult Human Bone Using Toluidine Blue. J Histotechnol 2005;28(2):73-9.

25. Preibisch S, Saalfeld S, Tomancak P. Globally optimal stitching of tiled 3D microscopic image acquisitions. Bioinformatics 2009;25(11):1463-5.

Commented [S3]: No Index Medicus entry

Commented [S4]: No IM entry

Commented [S5]: No IM entry. Abbrev. from NLM Catalog

Commented [S6]: No IM entry. Abbrev. from ISO 4

26. Schindelin J, Arganda-Carreras I, Frise E, Kaynig V, Longair M, Pietzsch T, et al. Fiji: an open-source platform for biological-image analysis. Nat Meth 2012;9(7):676-82.

27. Rohlf FJ. TPS Series. Department of Ecology and Evolution, State University of New York at Stony Brook: Stony Brook, 2010.

28. Hammer Ø, Harper DAT, Ryan PD. PAST: paleontological statistics software package for education and data analysis. Paleontol Electron 2001;4(9):9.

29. Crampton JS, Haines AJ. Users' Manual for Programs HANGLE, HMATCH, and HCURVE for the Fourier Shape Analysis of Two-Deminsional Outlines. Lower Hutt, New Zealand: Institute of Geological & Nuclear Sciences Ltd.; 1996 Oct. Report No.: 96/37.

30. Raum R. Resample. 1.0 ed. New York: NYCEP Morphometrics Group; 2006.

31. Klingenberg CP. MorphoJ: an integrated software package for geometric morphometrics. Mol Ecol Resour 2011;11(2):353-7.

32. Lynnerup N, Frohlich B, Thomsen JL. Assessment of age at death by microscopy: Unbiased quantification of secondary osteons in femoral cross sections. Forensic Sci Int 2006;159, Supplement:S100-S3.

33. Rose DC, Agnew AM, Gocha TP, Stout SD, Field JS. Technical note: The use of geographical information systems software for the spatial analysis of bone microstructure. Am J Phys Anthropol 2012;148(4):648-54.

34. Pfeiffer S, Lazenby R, Chiang J. Cortical remodeling data are affected by sampling location. Am J Phys Anthropol 1995;96(1):89-92.

35. Tersigni MA. Serial long bone histology: Inter- and intra-bone age estimation [dissertation]. Knoxville (TN): Univ. of Tennessee, 2005.

36. Chan AHW, Crowder CM, Rogers TL. Variation in cortical bone histology within the human femur and its impact on estimating age at death. Am J Phys Anthropol 2007;132(1):80-8.

Commented [S7]: ?

Commented [S8]: ?

37. Grivas CR, Komar DA. Kumho, Daubert, and the Nature of Scientific Inquiry: Implications for Forensic Anthropology. J Forensic Sci 2008;53(4):771-6.

38. Christensen AM, Crowder CM. Evidentiary Standards for Forensic Anthropology. J Forensic Sci 2009;54(6):1211-6.

39. The Law Commission. Expert evidence in criminal proceedings in England and Wales. London: The Stationary Office; 2011.

Commented [S9]: ?

Additional information and reprint requests:

Scott Dillon M.Sci.

Centre for Anatomy and Human Identification

Medical Sciences Institute

University of Dundee

Dundee, Scotland

DD1 5EH

Email: scott.dillon92@gmail.com

Statistic	Osteon Group									
	A	B	C	D	E	G	F	H	I	J
F	0.312	0.118	1.910	1.851	1.410	1.433	0.930	0.157	1.142	0.436
p	0.862	0.992	0.171	0.173	0.269	0.268	0.470	0.976	0.227	0.761

TABLE 1–*Results of repeated one-way permutation ANOVAs of Procrustes distances between groups of osteon digitisations replicated with random starting positions*

		Osteon Group								
		A	B	C	D	E	F	G	H	I
Osteon Group	B	0.008								
	C	0.006	0.008							
	D	0.008	0.008	0.003						
	E	0.007	0.004	0.007	0.008					
	F	0.009	0.005	0.006	0.008	0.006				
	G	0.008	0.008	0.008	0.008	0.006	0.007			
	H	0.007	0.003	0.006	0.006	0.007	0.009	0.007		
	I	0.007	0.007	0.004	0.009	0.008	0.009	0.009	0.007	
	J	0.0001	0.008	0.004	0.008	0.005	0.005	0.006	0.001	0.007

TABLE 2–*Results of a permutation test of pairwise distances between osteon groups with 10,000 iterations. Data represent p values*

Sampling site	n	CV1		CV2		Centroid size		
		$\bar{x}$	σ	$\bar{x}$	σ	$\bar{x}$	σ	Range
Proximal	217	-0.600	0.912	-0.587	0.992	21.501	0.440	2.077
Midshaft	164	1.335	1.212	-0.233	0.905	21.565	0.370	1.821
Distal	163	-0.544	0.866	0.805	1.097	21.717	0.357	1.936

TABLE 3–*Descriptive statistics relating to shape data (canonical variate scores) and centroid size of measured secondary osteons according to sampling site*

Pairwise Comparison		
	Midshaft	Distal
Proximal	0.0378	0.0397
Distal	0.0351	

TABLE 4–*Summary of p values resultant from a permutation test of pairwise Procrustes distances between diaphyseal sampling sites with 10,000 iterations*

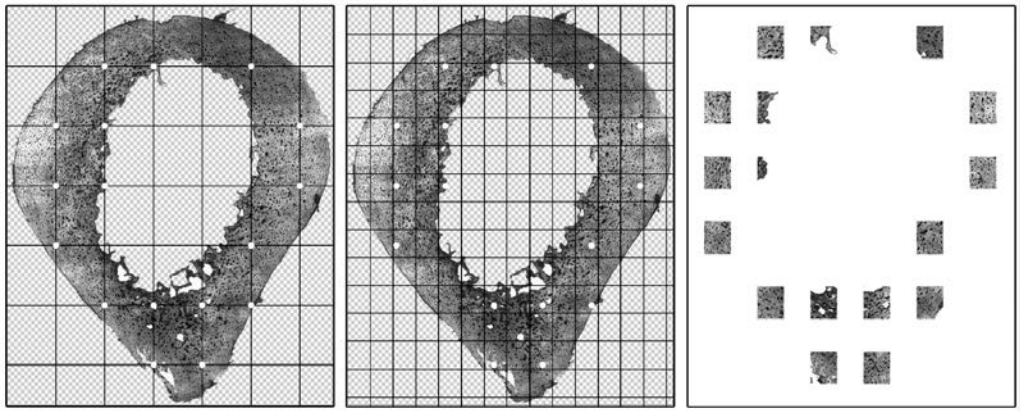

FIG. 1–*Overview of novel intra-sectional sampling protocol. (a) 15% width grid overlay. Grid intersections which cross the cortical bone are marked; (b) 7% width grid overlay; (c) All grid squares which contain an original intersection marker are extracted. All qualifying structures within extracted fields are subsequently analysed*

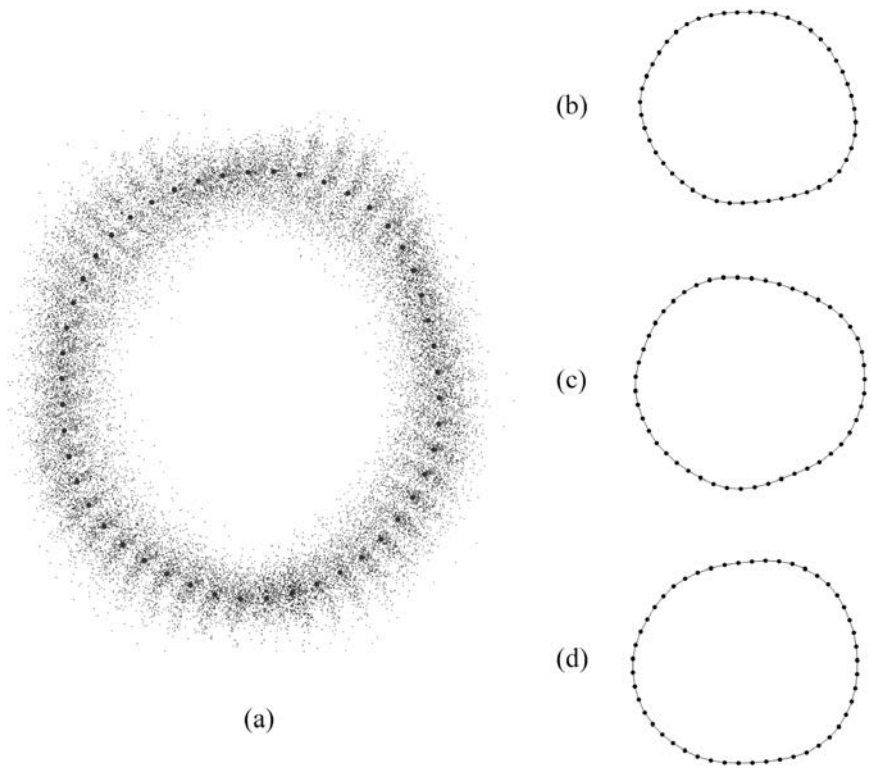

FIG. 2–*(a) Visualisation of Procrustes co-ordinates independent of sampling site as spread around landmark point means; (b) Mean shape of osteons exhibited within the proximal site after GPA; (c) Mean shape of osteons exhibited within the midshaft site after GPA; (d) Mean shape of osteons exhibited within the distal site after GPA*

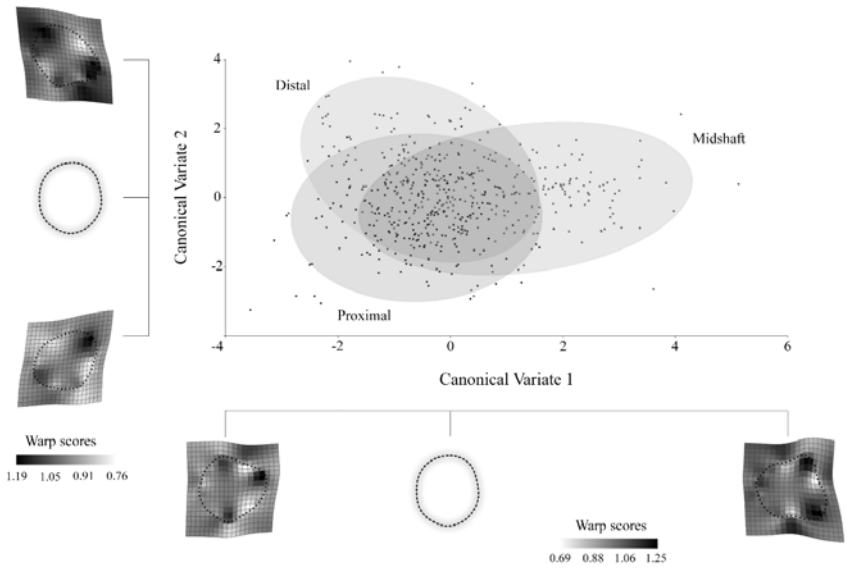

FIG. 3–*Canonical variate scores of measured osteons with sampling site as a grouping variable, displaying 95% confidence ellipses for groups and transformation grids illustrating shape change between extremes of the canonical axes as compared to the mean shape (origin)*

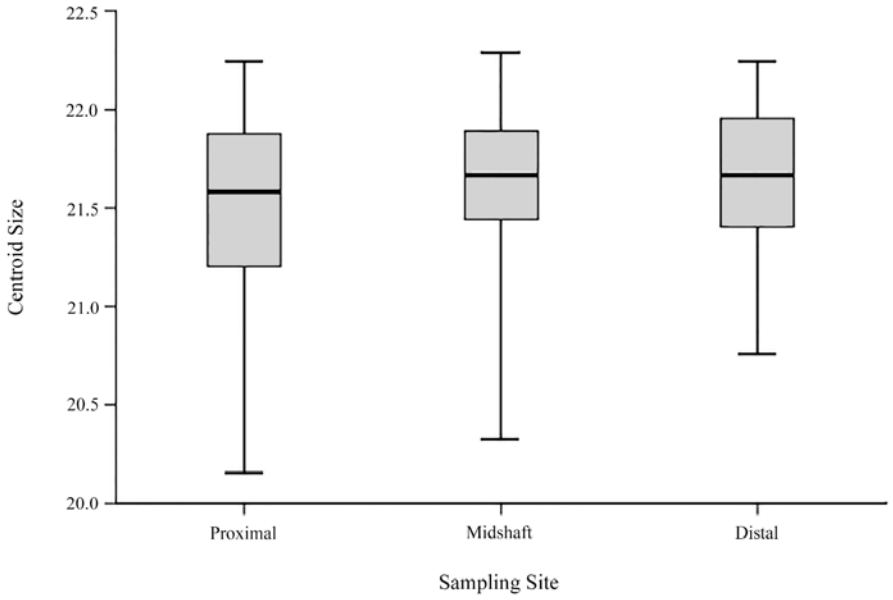

FIG. 4–*Box plot of centroid size according to sampling site*